

Electron paramagnetic resonance versus spin-dependent recombination: Excited triplet states of structural defects in irradiated silicon

L.S. Vlasenko

A.F. Ioffe Physico-Technical Institute, Russian Academy of Sciences, 194021, St. Petersburg, Russia

Yu.V. Martynov, T. Gregorkiewicz, and C.A.J. Ammerlaan

Van der Waals - Zeeman Laboratorium, Universiteit van Amsterdam, Valckenierstraat 65,

NL-1018 XE Amsterdam, The Netherlands

(Received 14 November 1994; revised manuscript received 1 March 1995)

Upon illumination some structural defects in irradiated silicon can be excited into the metastable triplet $S=1$ states. These triplet states can be involved in the excess-carriers recombination process. This paper provides a theoretical treatment of spin-dependent recombination (SDR) via an excited triplet state and reports on the properties of its electron-paramagnetic-resonance (EPR) spectrum detected by means of dc and microwave photoconductivity changes under magnetic-resonance conditions. The dependence of the spectral lines intensity on various experimental parameters (microwave power and phase, size of the sample) has been investigated and a comparison between the two techniques and the conventional EPR method has been made. Using the SDR technique the angular dependence of the line positions and intensities for the structural defects in their excited triplet states was studied and the spin-Hamiltonian parameters of the Si-PT1 and Si-PT4 spectra have been determined.

I. INTRODUCTION

The spin-dependent recombination (SDR) phenomenon was reported by Lepine.¹ He observed a change of the photoconductivity of a silicon sample when electron-paramagnetic-resonance (EPR) transitions were induced between magnetic sublevels of a recombination center. The conductivity was measured by applying electrical contacts to the sample which was placed in a microwave cavity and illuminated with band-gap light. Later SDR was also detected in Si/SiO₂ interfaces,² in plastically deformed silicon crystals,^{3,4} and in porous silicon.⁵ Based on the SDR via a phosphorus donor in bulk silicon the technique of magnetic field measurements has been proposed.⁶ The method has also been applied to detect structural defects in p - n junctions.⁷⁻¹¹ There it seems to be especially promising since in a p - n junction excess carriers can be injected electrically, which enables one to control their number and type.

In addition a similar, but contact-free, technique of the SDR-spectra detection has also been proposed.^{2,12-15} In this experimental scheme variations of the cavity Q factor reflect resonant changes in losses of the electric microwave field component due to the absorption by photoexcited free carriers. When applicable, this method appears to be more sensitive than conventional EPR by a few orders of magnitude. In the past it has served to detect several new spectra of the radiation defects in the excited triplet states Si-PT1,¹² Si-PT3,¹³ Si-PT4,¹⁴ and Si-PT5.¹⁵ In practice application of this method can hardly be distinguished from the usual EPR with illumination of the sample. Therefore under certain conditions when the concentration of defects is relatively high, both EPR and SDR can contribute to detectable signals and the problem

of their separation arises. However, the roles of electric and magnetic components of the microwave field are essentially different: The magnetic component induces an EPR transition while the electric component is used to detect the changes in photoconductivity. Therefore, the electric and magnetic components do not necessarily have to have the same frequency; i.e., the magnetic resonance can, for example, be induced at a radio frequency by means of a coil, while the detection of photoconductivity changes is carried out at a microwave frequency. Such an experiment has been performed.¹⁶ The SDR spectra of the shallow donors (P and As) were observed in low magnetic fields of the order of a few hundred gauss as well as the spectra of excited triplet states of radiation defects [spectra Si-PT1 and SL1 (Ref. 17)]. Moreover, even in the absence of the oscillating magnetic field the lines of photoconductivity changes were observed at the points of the anticrossing of the triplet state magnetic sublevels.^{13,14,18} These SDR results in low fields were later reproduced by Greulich-Weber.¹¹

Several models have been proposed in order to describe SDR quantitatively. In the model of Lepine¹ the recombination occurs via a center which is assumed to have an electron spin $S = 1/2$. The cross section of the recombination process depends on the spin polarizations of the carriers and the recombination centers. The saturation of EPR transitions of the centers diminishes their polarization and changes the recombination rate. This model cannot account for the magnitude of the SDR effect which appeared to be about 100 times stronger than the model predicted. In the approach of Kaplan *et al.*¹⁹ an electron and a hole are assumed to form a weakly bound pair which can have either a singlet or a triplet spin configuration. The triplet state has a longer lifetime

than the singlet and the transition to the singlet state is forbidden; therefore, an electron-hole pair in the triplet state can only dissociate without recombination. If due to an EPR transition the spin of either the electron or the hole is altered, the pair will be able to recombine. Recently a model describing SDR via a P_b center in silicon has been developed by Lannoo *et al.*²⁰ It provides a more elaborate treatment of the process as applied to that particular defect. A simple model of SDR via excited triplet states of radiation defects in silicon has been proposed in Ref. 13 and will be developed in more detail in the following section.

In practice optically detected magnetic resonance (ODMR) and SDR spectra are often observed in the same sample and from the same defect⁵ since the intensity of luminescence is also strongly connected with the recombination process.

The objective of this work was to investigate the main features of both the microwave- and dc-photoconductivity-based techniques of SDR detection and to make a comparison of these methods. Utilizing the SDR technique we were able to characterize some of the radiation-induced structural defects, involved in the carriers recombination process. Namely, we were able to determine spin-Hamiltonian parameters for the Si-PT1 and Si-PT4 spectra.

II. THEORETICAL ASPECTS

A. Probabilities of a triplet-singlet transition

Let us consider a hypothetical defect incorporating two electrons in two broken bonds in an external magnetic field. Their wave functions a and b will form odd and even linear combinations, i.e., bonding and antibonding orbitals $\eta = (a + b)/\sqrt{2}$ and $\xi = (a - b)/\sqrt{2}$. In the ground state both electrons will occupy the bonding orbital. A process of excitation and deexcitation of the defect, schematically depicted in Fig. 1, can serve as a recombination channel. The defect in the S_0 ground state can capture a photoexcited electron from the conduction

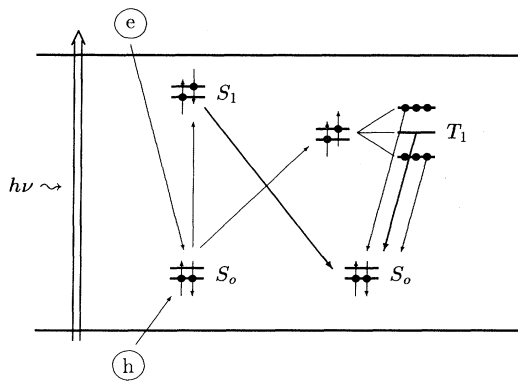


FIG. 1. Processes of the photoexcited carriers recombination via a hypothetical deep-level defect in silicon (see text for details).

band and a hole from the valence band. As a result the defect will go to an excited state. If this state is also a singlet (S_1), the defect almost immediately will relax to its ground state, thus accomplishing the act of carrier recombination and making itself available as a carrier trap. On the other hand, the excited triplet state (T_1) is metastable because the $T_1 \rightarrow S_0$ transition is forbidden. A spin-orbit coupling, however, partially allows the transition to the ground singlet state. The probability of this transition R^m is proportional to the square of the matrix element of the spin-orbit coupling operator \mathcal{H}_{SO} between the ground state S_0 and the sublevel T_1^m with spin projection m ($m = -1, 0, \text{ and } +1$):

$$R^m \sim |\langle S_0 | \mathcal{H}_{SO} | T_1^m \rangle|^2. \quad (1)$$

The wave functions S_0 and T_1^m can be chosen as follows:²¹

$$\begin{aligned} T_1^+ &= (1/\sqrt{2})(\eta_1\xi_2 - \eta_2\xi_1)\alpha_1\alpha_2, \\ T_1^0 &= (1/2)(\eta_1\xi_2 - \eta_2\xi_1)(\alpha_1\beta_2 + \alpha_2\beta_1), \\ T_1^- &= (1/\sqrt{2})(\eta_1\xi_2 - \eta_2\xi_1)\beta_1\beta_2, \\ S_0 &= (1/\sqrt{2})\eta_1\eta_2(\alpha_1\beta_2 - \alpha_2\beta_1), \end{aligned} \quad (2)$$

where α and β are the electron spin wave functions, corresponding to the positive and negative spin projections, respectively. The spin-orbit coupling operator is defined as

$$\mathcal{H}_{SO} = A(\vec{l}_1\vec{s}_1 + \vec{l}_2\vec{s}_2), \quad (3)$$

where \vec{l}_i is the angular momentum operator of the i th electron, \vec{s}_i is its spin momentum operator, and A is a scalar constant. The direct calculation of the matrix elements of this operator yields

$$\begin{aligned} \langle S_0 | \mathcal{H}_{SO} | T_1^\pm \rangle &= \frac{A\hbar}{2} (\langle \eta | l_x | \xi \rangle + i \langle \eta | l_y | \xi \rangle), \\ \langle S_0 | \mathcal{H}_{SO} | T_1^0 \rangle &= -\frac{A\hbar}{\sqrt{2}} \langle \eta | l_z | \xi \rangle; \end{aligned} \quad (4)$$

l_x , l_y , and l_z are defined in a coordinate frame connected with the magnetic field. Transforming them in the crystal coordinate frame for every magnetic field orientation one obtains angular dependences of the transition probabilities.

B. Kinetics of the recombination process via an excited triplet state

Let us consider a silicon sample illuminated by band-gap light. This illumination will produce excited carriers with the rate G . A carrier can be either captured by a defect in its ground state with the probability σ or recombine via some other channel with the probability \mathcal{R} . The carriers concentration n_e will be determined by these processes of generation and recombination. Suppose the concentration of the defect in the sample is n_D . A part of them with the concentration n_{S_0} is in the ground state, and the rest is in the excited triplet state. The population of the triplet state sublevels $|0\rangle$, $|+\rangle$, and $|-\rangle$ is

n^0 , n^+ , and n^- , respectively. The transitions $T_1^\pm \rightarrow S_0$ take place with the probability R , and the transition $T_1^0 \rightarrow S_0$ with the probability R^0 . The transitions between the magnetic sublevels can also occur with W as the spin relaxation rate (the Boltzmann polarization is being disregarded). If magnetic-resonance conditions are satisfied for the sublevels $|+\rangle$ and $|0\rangle$, the transitions between them occur with the probability \mathcal{B} . The whole system can then be described with the following set of equations:

$$n_D = n_{S_0} + n^+ + n^0 + n^-, \quad (5)$$

$$\frac{dn_e}{dt} = G - \sigma n_e n_{S_0} - \mathcal{R} n_e, \quad (6)$$

$$\frac{dn^+}{dt} = \frac{\sigma n_e n_{S_0}}{3} - n^+ R - (n^+ - n^0)(W + \mathcal{B}), \quad (7)$$

$$\frac{dn^0}{dt} = \frac{\sigma n_e n_{S_0}}{3} - n^0 R^0 - (2n^0 - n^+ - n^-)W - (n^0 - n^+) \mathcal{B}, \quad (8)$$

$$\frac{dn^-}{dt} = \frac{\sigma n_e n_{S_0}}{3} - n^- R - (n^- - n^0)W. \quad (9)$$

In the steady state, when external parameters are changing slowly and

$$\frac{dn^+}{dt} = \frac{dn^0}{dt} = \frac{dn^-}{dt} = 0, \quad (10)$$

the linear equations (7)–(9) can be solved together with respect to n^+ , n^0 , and n^- . Their sum will give the total concentration of the defects in the triplet state:

$$n^T = n^0 + n^+ + n^- = \frac{1}{3} \sigma n_e n_{S_0} F(\mathcal{B}), \quad (11)$$

where

$$F(\mathcal{B}) = \frac{(R + W)(2R^0 + R + 9W) + \mathcal{B}(R^0 + 5R + 9W)}{(R + W)(RR^0 + 2RW + R^0W) + \mathcal{B}(RR^0 + 2RW + R^0W + R^2)}. \quad (12)$$

From (5) and (6) follows

$$G = \frac{\sigma n_e n_D}{1 + \frac{1}{3} \sigma n_e F(\mathcal{B})} + \mathcal{R} n_e. \quad (13)$$

Solving the square equation (13) with respect to n_e we obtain the concentration of the free carriers. The SDR signal is proportional to the change of the carriers concentration when the system is brought in the magnetic-resonance conditions and \mathcal{B} changes from 0 to some finite value. Since n_e is a function of R and R^0 , whose values depend on the direction of the magnetic field, as has been shown in the previous subsection, the magnitude of the SDR signal is also expected to be angular dependent.

III. EXPERIMENT

The material used in the SDR experiments was high-resistivity (300 Ω cm) float-zoned n -type phosphorus-doped silicon. The samples were cut along a $\langle 110 \rangle$ crystalline direction from a $\langle 111 \rangle$ -oriented silicon slice of ≈ 0.7 mm thickness and irradiated by 1-MeV electrons to a number of doses from 10^{16} to 10^{18} cm $^{-2}$. dc and microwave SDR measurements were performed in an X -band superheterodyne spectrometer equipped with a cylindrical TE $_{011}$ cavity, placed in a stainless-steel helium cryostat, and with the magnetic-field modulation at 12.3 Hz. The sample was illuminated via a quartz rod by a high-pressure 200-W xenon lamp. Due to a considerable heat input caused by the lamp, the temperature of the measurements was slightly elevated and was about 15 K. In the experiment the magnet could be rotated, allowing the position of the sample to be kept constant with

respect to the light source.

In the microwave-photoconductivity experiment the sample was displaced by about a quarter of the radius from the axis of the cavity in order to have it in a position where both the electric and magnetic components of the microwave field are nonzero.

In the dc-photoconductivity experiment the sample was mounted in the center of the cavity directly on the quartz lightguide. In order to ensure good Ohmic contact two opposite $\langle 211 \rangle$ surfaces of the sample were covered by metallic indium and two copper wires were pressed against these surfaces. The sample was serially connected with a load resistor, tuned to have the same resistance as the sample. A direct current was passed through this circuit and changes of the voltage drop across the sample were detected by a lock-in amplifier.

IV. EXPERIMENTAL RESULTS

The SDR spectra typically observed in the course of this study are depicted in Fig. 2. These are the Si-PT1 and Si-PT4, reported earlier.^{12,14} The intensity of the Si-PT1 spectrum was much higher than that of Si-PT4; therefore Si-PT1 has been chosen as the subject of the detection conditions study, described in the following subsection. We were also able to obtain a conventional-EPR spectrum of this defect. This allowed for a direct comparison of sensitivities of the EPR and SDR methods.

For the samples, whose size was large enough to ensure an optimal cavity filling factor, the microwave method of detection SDR appeared to be more sensitive than the dc measurements. This is in contrast to the other SDR results.^{11,22} We attribute this fact to an extremely high

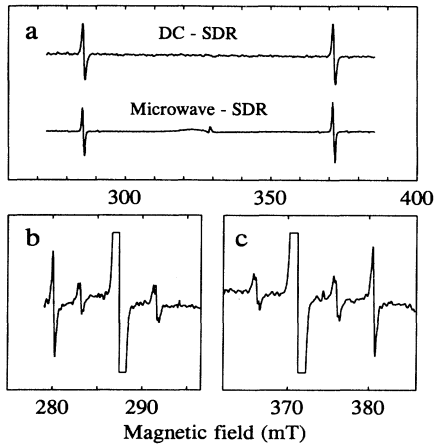


FIG. 2. EPR spectra in electron-irradiated silicon. (a) spectrum Si-PT1, detected by dc- and microwave-photoconductivity variations; (b) and (c): enlarged parts of spectrum Si-PT1 with ^{29}Si hyperfine satellites. Sharp lines at 280 and 381 mT belong to the spectrum Si-PT4.

sensitivity of our X-band spectrometer,²³ since, in fact, in the case of a microwave SDR experiment the detection part of an EPR spectrometer is being utilized. Moreover, it appeared that resonance lines were broader in case of the dc SDR, while for the microwave method of detection the linewidth was equal to that of an EPR line.

Dependences of the signals on various experimental parameters are outlined below in detail.

A. SDR signal detection conditions

1. Dispersion and absorption

Although, as we have already pointed out, an SDR experiment resembles very much a standard photo-EPR measurement, there are a few important differences in the conditions for these two experiments. The dispersion component is always present in the EPR signal. Moreover, when the EPR transition is saturated this component becomes much stronger than the absorption part. However, microwave-SDR signals were only observable when our spectrometer was tuned to absorption. The dispersion signal was at least two orders of magnitude weaker than absorption.

To explain this fact let us consider an electron gas affected by a periodic electrostatic field $\mathbf{E} = E \exp(-i\omega t)$. Its conductance σ (see, for example, Ref. 24) is given by

$$\begin{aligned} \sigma(\omega) &= \frac{\sigma_0}{1 - i\omega\tau}, \\ \sigma_0 &= \frac{ne^2\tau}{m^*}, \end{aligned} \quad (14)$$

where n is the concentration of electrons, m^* is their effective mass, e is their charge, and τ is an average time between two scattering events. The dielectric constant ϵ of such a gas is

$$\epsilon(\omega) = 1 + \frac{4\pi i\sigma}{\omega} = \epsilon'(\omega) + i\epsilon''(\omega), \quad (15)$$

where

$$\epsilon'(\omega) = 1 - \frac{4\pi ne^2}{m^*[\omega^2 + (1/\tau^2)]}$$

and

$$\epsilon''(\omega) = \frac{4\pi ne^2}{m^*\omega\tau[\omega^2 + (1/\tau^2)]}.$$

When the concentration of carriers changes, the corresponding change in ϵ' will produce a dispersion signal, whereas the change in ϵ'' will manifest itself in absorption. The dispersion signal is thus proportional to $d\epsilon'/dn$ and absorption to $d\epsilon''/dn$. The absorption to dispersion ratio will then be

$$\frac{(d\epsilon'/dn)}{(d\epsilon''/dn)} = \omega\tau. \quad (17)$$

Since in our experiment $\nu = \omega/2\pi$ is of the order of 9 GHz and τ for the temperature of 15 K is approximately 0.7×10^{-13} s, this ratio appears to be about 4×10^{-3} . The $\omega\tau$ quantity is known to play a key role in the observation of the cyclotron resonance. Control experiments on unirradiated silicon crystals have shown that the signal of cyclotron resonance in this material drops dramatically when the temperature rises from 1.7 to 15 K.

2. Dependence on the microwave power

Another characteristic feature of the microwave-detected SDR signals is their anomalous dependence on the incident microwave power. A signal of conventional EPR is proportional to the number of transitions between the magnetic sublevels. In the absence of saturation this number grows as the square of the magnetic component of the microwave field, i.e., as the incident microwave power P . A voltage from a linear detector is proportional to the square root of power; therefore an EPR signal is proportional to \sqrt{P} . At higher power when the transition is saturated, the EPR signal does not depend on the power. Figure 3 presents a dependence of the Si-PT1 spectrum line intensities on microwave power. This dependence appears to be quadratic for low power levels and becomes linear when the power is high, contrary to what one would expect for an EPR signal.

In case of microwave SDR the variation of the power absorbed by free carriers is proportional to the change of their concentration times the square of the electric field component. Since, for the small values of P , the change in the carriers concentration depends linearly on the number of EPR transitions, the signal from a linear detector will be proportional to P . Even when the EPR transition is heavily saturated, the microwave-SDR signal will still be growing as \sqrt{P} because the amplitude of the E component is increasing. For dc SDR the saturation was observable (see Fig. 4) since in this case the signal

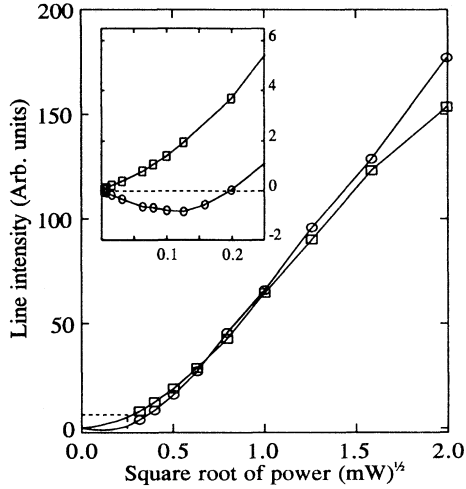


FIG. 3. Line intensity dependence of the Si-PT1 microwave-detected SDR spectrum on the microwave power. \circ , low-field line; \square , high-field line. $\vec{B} \parallel \langle 111 \rangle$, $T=15$ K, $\nu = 9.213\,648$ GHz.

does not depend on the E component of the microwave field.

3. Dependence on the size of the sample

We have performed measurements on samples of different sizes, exposed to the same dose of irradiation under the same experimental conditions, applying both the microwave and dc technique of detection. We have found that while the microwave-SDR signal magnitude is proportional to the volume of the sample, the dc-SDR signal has the same magnitude for the samples whose volumes

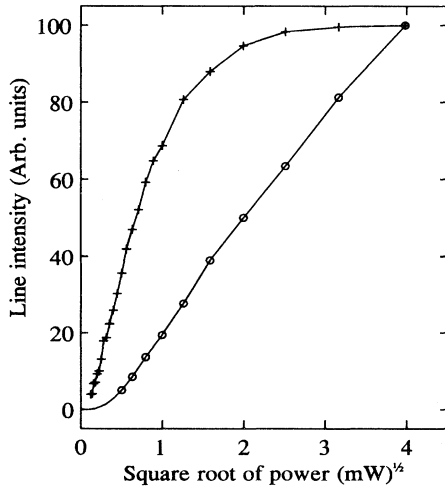


FIG. 4. Saturation curves of the Si-PT1 low-field spectrum line, detected by means of the microwave- (\circ) and dc- ($+$) photoconductivity variations. $\vec{B} \parallel \langle 111 \rangle$, $T=15$ K, $\nu = 9.213\,648$ GHz.

differ by an order of 10. Such a rather unexpected result can, however, easily be understood. In case of the microwave-SDR experiment the signal occurs as a result of the electric-field-component absorption by free carriers. This signal is proportional to the total number of the carriers, i.e., to the product of their concentration and the volume of the sample. In case of a dc-SDR experiment the situation is different. The resistivity of the sample is given by

$$R = \frac{l}{S\sigma}, \quad (18)$$

where l is the distance between the electric contacts, S is their surface, and σ is the conductivity of the sample. Because the sample is serially connected with a load, the voltage drop across the sample is

$$U = \frac{U_0 R}{R + R_L}, \quad (19)$$

where U_0 is the power supply voltage, and R_L is the value of the load resistor. In our experiment we used $U_0 = 1.5$ V and $R_L \approx 1$ M Ω . A voltage response to a small change of the conductivity $\Delta\sigma$ will in this case be

$$\Delta U = -\frac{\Delta\sigma U_0 S}{l(1 + R_L/R)^2}. \quad (20)$$

If we choose R_L equal to R in order to have the maximal response and take into account (18), we arrive at

$$\Delta U = -U_0 \frac{\Delta\sigma}{4\sigma}. \quad (21)$$

The voltage response appears to be independent from the size of the sample, provided of course that the latter remains sufficiently large to be treated macroscopically. In our experiment we estimated the maximal value of $\Delta\sigma/\sigma$ to be $\approx 5 \times 10^{-3}$. The detection limit of the method in our case was approximately two orders of magnitude lower than this value.

B. EPR results

In a sample exposed to a relatively high ($\sim 10^{18}$ cm $^{-2}$) irradiation dose a conventional EPR spectrum of the Si-PT1 defect has been observed. The detection of the EPR spectrum was possible only at extremely low microwave power levels of ≈ 10 μ W. As can be seen from Fig. 5 this spectrum is observable both in absorption and dispersion and the magnitude of the signal is in both modes approximately the same. The phases of high- and low-field lines of the spectrum are opposite. The low- and high-field lines correspond to absorption and to emission of the microwave power, respectively. This feature is typical for an EPR spectrum of a defect in an excited triplet state and was, for example, observed for the oxygen-vacancy complex.¹⁷ At higher microwave power both lines have the same phase and are detectable only in absorption mode.

Both EPR and SDR line intensities are strongly angular dependent. The experimental points could only be measured in a relatively small range of angles close to

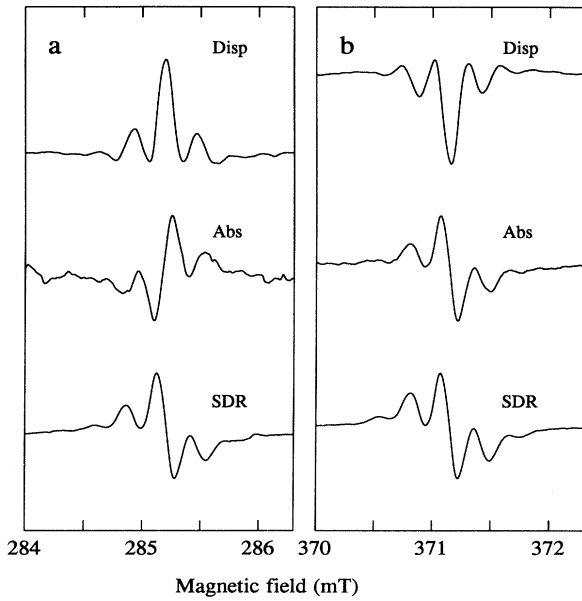


FIG. 5. Low- (a) and high- (b) field lines of Si-PT1 detected under conditions of the conventional EPR, in dispersion and absorption modes, and by microwave photoconductivity changes. Gain for EPR signals is 10^3 times higher than for SDR. EPR signals were detected with a microwave power at the level of $\approx 10 \mu\text{W}$, the power level for the SDR signal is $\approx 1 \text{ mW}$. $\vec{B} \parallel \langle 111 \rangle$, $T=15 \text{ K}$, $\nu=9.213558 \text{ GHz}$.

[111]. Fitting of such incomplete angular dependences has a high degree of uncertainty and is somewhat speculative. Nevertheless, we were able to determine the symmetry of the Si-PT1 and Si-PT4 defects and to obtain their spin-Hamiltonian parameters, assuming that both spectra are associated with an $S = 1$ state and that the two lines belong to two transitions $m : \pm 1 \leftrightarrow 0$.

An angular dependence of the magnetic resonance field for the Si-PT1 spectrum is plotted in Fig. 6. These data can be fitted with a spin Hamiltonian of trigonal symmetry, including an electron-Zeeman, a fine-structure, and a hyperfine-structure terms in the following form:

$$\mathcal{H}_{\text{Si-PT1}} = \mu_B \vec{B} \cdot \mathbf{g} \cdot \vec{S} + \frac{D}{3} \vec{S} \cdot \vec{S} + \vec{S} \cdot \mathbf{A}^{\text{Si}} \cdot \vec{I}^{\text{Si}}, \quad (22)$$

where the symbols have their usual meaning.²⁵ The parameters are found to be $g_{\parallel} = 2.0076$, $g_{\perp} = 2.003$, and $D = \pm 1207 \text{ MHz}$. The values of the parameters g_{\parallel} and D could be established very accurately since they are only determined by the line positions in the $\langle 111 \rangle$ direction that are well measured. The hyperfine splitting (see Fig. 2) arises from interaction with one ^{29}Si nucleus ($I = 1/2$, 4.7% abundance) and for $\vec{B} \parallel \langle 111 \rangle$ the hyperfine-constant value $A^{\text{Si}} = 285 \text{ MHz}$ could be estimated. As can also be seen from Fig. 7, extra splitting due to the interactions with more distant silicon nuclei is observable and results in a complicated lineshape.

Under similar assumptions as for Si-PT1, the angular dependence of the Si-PT4 spectrum (see Fig. 8) could be

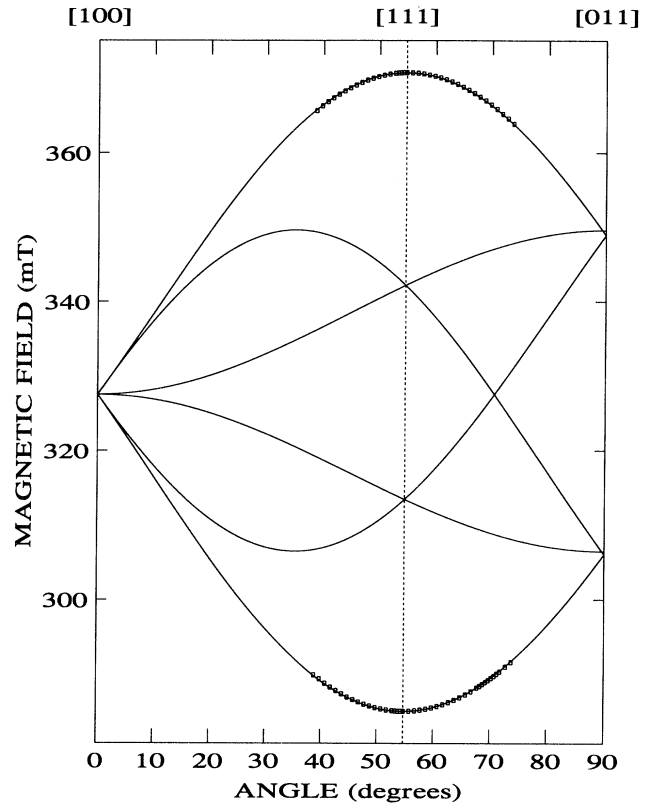


FIG. 6. Angular dependence of resonance field of the Si-PT1 spectrum. \square , experiment; solid lines, computer fit. $T=15 \text{ K}$, $\nu=9.213648 \text{ GHz}$.

fitted with the following spin Hamiltonian of monoclinic symmetry:

$$\mathcal{H}_{\text{Si-PT4}} = \mu_B \vec{B} \cdot \mathbf{g} \cdot \vec{S} + \vec{S} \cdot \mathbf{D} \cdot \vec{S}. \quad (23)$$

The parameters of this spin Hamiltonian are summarized in Table I.

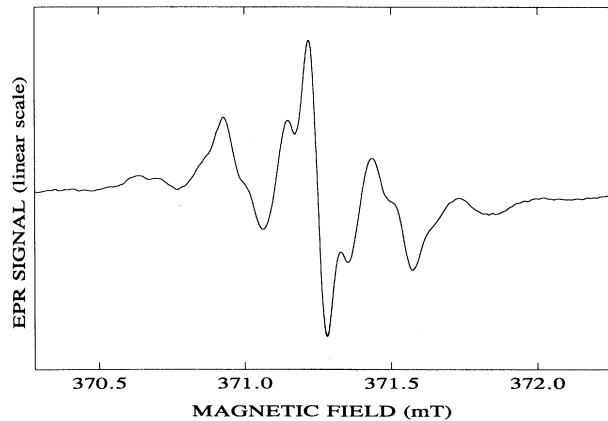


FIG. 7. Detailed scan of the high-field Si-PT1 spectrum line, taken by means of microwave-detected SDR. $\nu = 9.216294 \text{ GHz}$, $T=15 \text{ K}$.

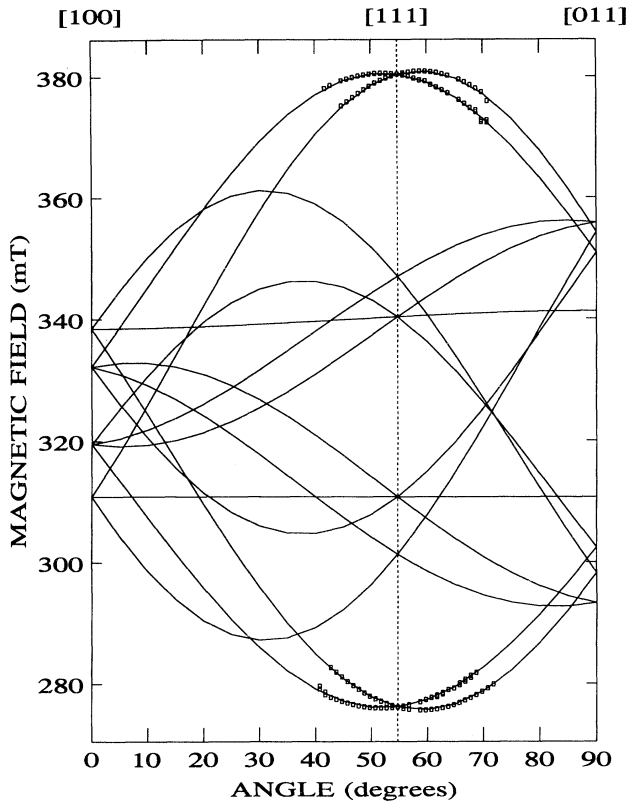


FIG. 8. Angular dependence of resonance field of the Si-PT4 spectrum. \square , experiment; solid lines, computer fit. $T=15$ K, $\nu=9.2163$ GHz.

V. DISCUSSION OF EPR RESULTS

It has been suggested that the Si-PT1 SDR spectrum and luminescence with zero-phonon line at 0.97 eV arise from the same defect.²⁶ According to the results of an ODMR study on this luminescence band the symmetry of the defect is monoclinic at 1.7 K but at the elevated temperature of ≈ 30 K the motional averaging yields a trigonal spectrum whose spin-Hamiltonian parameters²⁷ are very close to those of the Si-PT1 defect, reported here (see Table II). In Ref. 27 an interstitial silicon atom bonded to two adjacent substitutional carbon atoms has been proposed as a model of the 0.97-eV-luminescence-associated defect. Since the interstitial

TABLE I. Spin-Hamiltonian parameters of the Si-PT4 spectrum as obtained from the analysis with effective spin $S = 1$. Eigenvector \bar{n}_2 for both tensors is parallel to the [011] direction; vector \bar{n}_1 is not far from [111] and makes an angle θ with [011]. Absolute signs of the D -tensor principal values cannot be determined in an EPR or SDR experiment.

Tensor	Principal values			Angle θ (deg)
	T_1	T_2	T_3	
\mathbf{g}	2.005	2.012	2.027	≈ 34
\mathbf{D}	± 984 MHz	∓ 286 MHz	∓ 698 MHz	≈ 31

TABLE II. The values of the Si-PT1 spin-Hamiltonian parameters compared to the parameters of the trigonal spectrum of the 0.97 eV luminescence line defect. The latter values were found by averaging the parameters of the monoclinic defect, reported in Ref. 27, over three equivalent C_{1h} distortions.

Defect	g_{\parallel}	g_{\perp}	D (MHz)	$A^{\text{Si}}(\bar{B} \parallel \langle 111 \rangle)$ (MHz)
Si-PT1	2.0076	2.003	1207	285
Defect associated with the 0.97-eV luminescence line	2.004	2.003	1201	308

atom can hop between three equivalent monoclinic distortions and at higher temperature (when the frequency of hopping becomes higher than the characteristic measuring frequency), a motionally averaged trigonal spectrum emerges.

We observe the Si-PT1 spectrum at a temperature lower than 30 K, reported in Ref. 27. One might try to ascribe this fact to the difference in the measuring frequency (X band in the current work versus Q band in Ref. 27). Indeed, in another study on γ -irradiated silicon diodes, also performed in X band, Yan *et al.* have observed a trigonal ODMR spectrum with the parameters similar to that of Si-PT1, coming from the 0.97-eV zero-phonon luminescence line.²⁸ However, our control measurements in a K -band spectrometer at ≈ 6 K have also revealed only the trigonal Si-PT1 spectrum. It is then more likely to assume that, contrary to the samples used in the present experiment, the materials of Ref. 27 contained a substantial amount of internal strain. It is this strain that “freezes” the 0.97-eV-luminescence-related defect in monoclinically distorted configurations and makes the barrier for reorientation higher.

If we assume that Si-PT1 and the 0.97-eV-luminescence-related defects are identical, we can calculate angular dependences of the transition probabilities

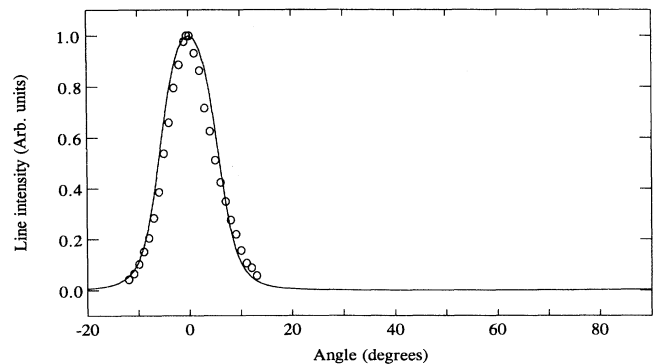


FIG. 9. Angular dependence of the Si-PT1 SDR spectrum line intensity. \circ , experiment; solid line, computer simulation. The values of the parameters are $n_D = 1 \times 10^{14} \text{ cm}^{-3}$, $n_e = 3.4 \times 10^8 \text{ cm}^{-3}$, $\sigma = 1 \times 10^{-8} \text{ cm}^3 \text{ s}^{-1}$, $G = 1 \times 10^{13} \text{ cm}^{-3} \text{ s}^{-1}$, $\mathcal{R} = 2 \times 10^3 \text{ s}^{-1}$, $B/C = 1 \times 10^{-4}$, $W/C = 9 \times 10^{-2}$.

from its T_1^m magnetic sublevels to the ground state S_0 . We choose the Z axis of the defect-related coordinate frame in such a way that it will coincide with a $\langle 111 \rangle$ crystalline direction. P_x and P_y silicon orbitals can be chosen as one-electron wave functions a and b . Then bonding and antibonding orbitals will be $\eta = (P_x + P_y)/\sqrt{2}$ and $\xi = (P_x - P_y)/\sqrt{2}$. Using the formulas (4) we obtain

$$\begin{aligned} R &\sim \frac{A^2 \hbar^4}{4} \sin^2 \phi = \frac{C}{2} \sin^2 \phi, \\ R^0 &\sim \frac{A^2 \hbar^4}{2} \cos^2 \phi = C \cos^2 \phi, \end{aligned} \quad (24)$$

with C as a constant and ϕ as the angle between the direction of the magnetic field and a $\langle 111 \rangle$ crystalline axis. Using formulas (11)–(13) and (24) we have simulated an angular dependence of the SDR signal intensity (see Fig. 9). Although the combination of the values of the parameters is not unique, the simulation seems to describe the experiment. Despite many attempts we were not able to detect SDR lines in other directions of the magnetic field.

VI. CONCLUSIONS

We have presented a theoretical treatment of the spin-dependent recombination of photoexcited carriers via an excited triplet state of a defect center. The dc and microwave variations of the SDR technique have been discussed and compared. The technique has been subsequently applied to study Si-PT1 and Si-PT4 radiation defects in silicon. For the Si-PT1 center the signal detection conditions have been investigated. We have found that the intensity of the spectral lines, measured by means of microwave SDR in the absence of saturation, depends quadratically on the microwave power, contrary to a conventional EPR, where this dependence is known to be linear. It has also been found that the dc-SDR line intensity does not depend on the size of the sample. Further, the angular dependences of the resonance magnetic field for the Si-PT1 and Si-PT4 defects has been studied and the parameters of their spin Hamiltonians have been determined. Following the current results it has been suggested that the Si-PT1 defect is also responsible for the 0.97-eV zero-phonon line luminescence.

-
- ¹ D. J. Lepine, Phys. Rev. B **6**, 436 (1972).
² G. Mendz, D. J. Miller, and D. Haneman, Phys. Rev. B **20**, 5246 (1979).
³ L. S. Mima, V. I. Strikha, and O. V. Tretyak, Sov. Phys. Semicond. **14**, 1328 (1980).
⁴ V. V. Kveder, Yu. A. Osip'yan, and A. I. Shalynin, Sov. Phys. JETP **56**, 389 (1982).
⁵ M. S. Brandt and M. Stutzmann, Appl. Phys. Lett. **61**, 2569 (1992).
⁶ A. Honig and M. Moroz, Rev. Sci. Instrum. **49**, 183 (1978).
⁷ I. Solomon, Solid State Commun. **20**, 215 (1976).
⁸ F. I. Borisov, V. I. Strikha, and O. V. Tretyak, Sov. Phys. Semicond. **15**, 1149 (1981).
⁹ F. Rong, E. H. Poindexter, M. Harmatz, W. R. Buchwald, and G. J. Gerardi, Solid State Commun. **76**, 1083 (1990).
¹⁰ P. Christmann, M. Bernauer, C. Wetzl, A. Asenov, B. K. Meyer, and A. Endrös, Mater. Sci. Forum **83-87**, 1165 (1992).
¹¹ S. Greulich-Weber, Mater. Sci. Forum **143-147**, 1337 (1994).
¹² L. S. Vlasenko, M. P. Vlasenko, and V. A. Khramtsov, Sov. Tech. Phys. Lett. **10**, 646 (1984).
¹³ L. S. Vlasenko, M. P. Vlasenko, V. N. Lomasov, and V. A. Khramtsov, Sov. Phys. JETP **64**, 612 (1986).
¹⁴ L. S. Vlasenko, in *The Physics of Semiconductors*, edited by E. M. Anastassakis and J. D. Joannopoulos (World Scientific, Singapore, 1990), p. 714.
¹⁵ M. P. Vlasenko and L. S. Vlasenko, Sov. Phys. Solid State **33**, 1326 (1991).
¹⁶ L. S. Vlasenko and V. A. Khramtsov, Sov. Phys. Semicond. **20**, 688 (1986).
¹⁷ K. L. Brower, Phys. Rev. B **4**, 1968 (1971).
¹⁸ L. S. Vlasenko and V. A. Khramtsov, JETP Lett. **42**, 38 (1985).
¹⁹ D. Kaplan, I. Solomon, and N. F. Mott, J. Phys. (Paris) Lett. **39**, L-51 (1978).
²⁰ M. Lannoo, D. Stievenard, D. Deresmes, and D. Vuillaume, Mater. Sci. Forum **143-147**, 1359 (1994).
²¹ S. P. McGlynn, T. Azumi, and M. Kinoshita, *Molecular Spectroscopy of the Triplet State* (Prentice-Hall, Englewood Cliffs, NJ, 1969).
²² S. Greulich-Weber (private communication).
²³ H. E. Altink, T. Gregorkiewicz, and C. A. J. Ammerlaan, Rev. Sci. Instrum. **63**, 5742 (1992).
²⁴ N. W. Ashcroft and N. D. Mermin, *Solid State Physics* (Holt, Rinehart, and Wilson, New York, 1976).
²⁵ A. Abragam and B. Bleaney, *Electron Paramagnetic Resonance of Transition Ions* (Clarendon, Oxford, 1970).
²⁶ G. D. Watkins (private communication).
²⁷ K. P. O'Donnell, K. M. Lee, and G. D. Watkins, Physica **116B**, 258 (1983).
²⁸ M. X. Yan, K. P. Homewood, and B. C. Cavenett, J. Phys. C **19**, L189 (1986).